THE ASTROPHYSICAL JOURNAL, 536:173–184, 2000 June 10

STAR FORMATION RATES IN DISK GALAXIES AND CIRCUMNUCLEAR STARBURSTS FROM CLOUD COLLISIONS

JONATHAN C. TAN
Department of Astronomy, University of California, Berkeley, CA 94720; jt@astron.berkeley.edu
Received 1999 June 22; accepted 2000 January 26

ABSTRACT

We invoke star formation triggered by cloud-cloud collisions to explain global star formation rates of disk galaxies and circumnuclear starbursts. Previous theories based on the growth rate of gravitational perturbations ignore the dynamically important presence of magnetic fields. Theories based on triggering by spiral density waves fail to explain star formation in systems without such waves. Furthermore, observations suggest gas and stellar disk instabilities are decoupled. Following Gammie, Ostriker, & Jog, the cloud collision rate is set by the shear velocity of encounters with initial impact parameters of a few tidal radii, due to differential rotation in the disk. This, together with the effective confinement of cloud orbits to a two-dimensional plane, enhances the collision rate above that for particles in a three-dimensional box. We predict $\Sigma_{\rm SFR}(R) \propto \Sigma_{\rm gas}\,\Omega(1-0.7\beta)$. For constant circular velocity ($\beta = 0$), this is in agreement with recent observations by Kennicutt. Our estimates for the normalization of this star formation law, while uncertain, are consistent with the observed star formation in the Milky Way and starburst galaxies. We predict a B-band Tully-Fisher relation: $L_B \propto v_{\rm circ}^{7/3}$, also consistent with observations. As additional tests, we predict enhanced/reduced star formation in regions with relatively high/low shear rates, and lower star formation efficiencies in clouds of higher mass.

Subject headings: galaxies: spiral — galaxies: starburst — ISM: clouds — stars: formation

1. INTRODUCTION

Understanding how the global star formation rates (SFRs) of galaxies and starbursts depend on their physical properties is essential for an understanding of galaxy evolution. Furthermore, such knowledge can also reveal much about the star formation process itself.

Empirically, in disk galaxies (Kennicutt 1989, 1998, hereafter K89, K98) and the circumnuclear disks of starbursts (Downes & Solomon 1998, hereafter DS98), star formation occurs in regions where the gas disk is unstable to gravitational perturbation growth. This can be expressed as a condition on the surface density of gas:

$$\Sigma_{\rm gas} > \Sigma_{\rm crit} = \frac{\alpha\kappa\sigma_{\rm gas}}{\pi G} \equiv Q\Sigma_{\rm gas} \tag{1}$$

(Toomre 1964; Quirk 1972), where $\sigma_{\rm gas}$ is the gas velocity dispersion; α is a dimensionless constant near unity, to account for deviations of real disks from the idealized Toomre thin-disk, single-fluid model; Q is a dimensionless parameter; and κ is the epicyclic frequency:

$$\kappa = \sqrt{2}\,\frac{v_{\rm circ}}{R}\left(1 + \frac{R}{v_{\rm circ}}\,\frac{dv_{\rm circ}}{dR}\right)^{1/2} = \sqrt{2}\,\frac{v_{\rm circ}}{R}\,(1+\beta)^{1/2}\,. \tag{2}$$

Here $v_{\rm circ}$ is the circular velocity at a particular galactocentric radius R, and $\beta \equiv d\ln v_{\rm circ}/d\ln R$, which is zero for a flat rotation curve. From the outermost galactic star-forming regions, K89 finds $\alpha \simeq 0.67$, assuming $\sigma_{\rm gas} = 6$ km s^{-1}. The result $\alpha < 1$ is expected, because of the destabilizing influence of a stellar disk (Jog & Solomon 1984; Jog 1996). Where $Q < 1$, on scales around $\lambda_{\rm crit} = 2\pi\sigma_{\rm gas}/Q\kappa$, the gas disk is gravitationally unstable and fragments into bound clouds. When stars form, the energy they release raises $\sigma_{\rm gas}$, and star formation is hypothesized (e.g., Silk 1997) and observed (K89; DS98) to self-regulate, so that $Q \sim O(1)$.

All star formation is observed to occur in molecular clouds, and the majority in giant molecular clouds (GMCs), with masses $\gtrsim 10^5\ M_\odot$ (see Blitz & Williams 1999 and McKee 1999 for reviews). However, K89 reported the surprising result that the correlation of the SFR with the surface density of molecular gas was much weaker than with the total (atomic + molecular). Uncertainties in CO to H_2 conversion may account for some of the poor correlation; however, the data suggest that the immediate supply of gas controlling the SFR is both atomic and molecular. This implies that the atomic to molecular conversion timescale, $t_{\rm conv}$, is short compared to the timescale on which star formation is regulated. Spitzer (1978) finds the rate constant for molecule formation on dust grains to be approximately 2.0×10^{-17} cm^3 s^{-1}, for typical Galactic interstellar medium (ISM) metallicities. Ignoring destruction processes, a naive estimate of the time to convert a region with $n_{\rm H\,I} \sim 1000$ cm^{-3}, perhaps created from the collision of two atomic clouds, to H_2, gives $t_{\rm conv} \sim 2 \times 10^6$ yr, which is a relatively short timescale.

Where $Q \lesssim 1$, the SFR is observed to be correlated with gas density. Schmidt (1959) introduced the parameterization of the volume densities $\rho_{\rm SFR} \propto \rho_{\rm gas}^n$, with $n \sim 1$–2. By looking at about 100 different galactic and circumnuclear starburst disk systems, K98 found a similar relation for disk-averaged surface densities of gas and star formation, valid over 5 orders of magnitude in $\overline{\Sigma_{\rm gas}}$,

$$\overline{\Sigma_{\rm SFR}} \propto (\overline{\Sigma_{\rm gas}})^N\,, \tag{3}$$

with $N \sim 1.4 \pm 0.15$ (Fig. 1) (however, see Taniguchi & Ohyama 1998). K98 finds that the SFR is also correlated with the orbital angular frequency, Ω, via

$$\overline{\Sigma_{\rm SFR}} \propto \overline{\Sigma_{\rm gas}}\,\Omega \tag{4}$$

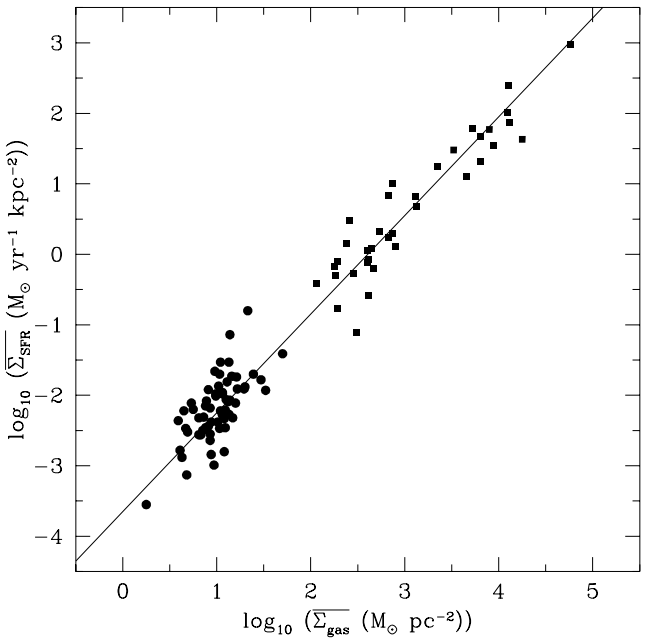

FIG. 1.—Classical Schmidt law: $\overline{\Sigma_{\rm SFR}} \propto (\overline{\Sigma_{\rm gas}})^N$, from Kennicutt (1998). Data are disk-averaged quantities for normal galactic disks (*filled circles*) and circumnuclear starburst disks (*filled squares*). The line is a least-squares fit with index $N = 1.40$. Systematic uncertainties between the normalization of the normal and starburst samples are of the order of a factor of 2.

(Fig. 2). Ω is measured at the outer radius of the star-forming region (see § 2.3.2).

Previous theories for explaining these relations fall into two broad categories, based either on the growth rate of gravitational perturbations in a disk or on the triggering of star formation in gas passing through spiral or bar density waves. In this paper we present a third paradigm, in which cloud collisions determine the SFR.

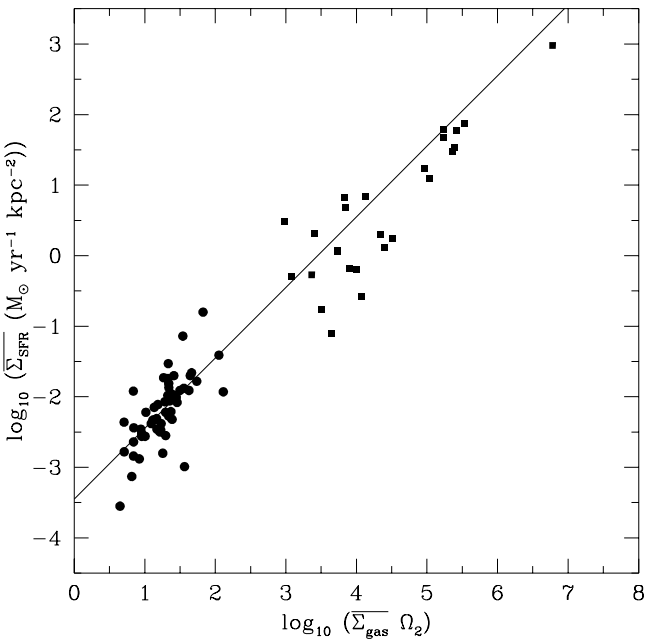

FIG. 2.—Modified Schmidt law: $\overline{\Sigma_{\rm SFR}} \propto \overline{\Sigma_{\rm gas}}\,\Omega_2$ from Kennicutt (1998). Data are disk-averaged quantities for normal galactic disks (*filled circles*) and circumnuclear starburst disks (*filled squares*). The line is a median fit to the normal galactic disk sample, with the slope fixed at unity as predicted by eq. (23). Systematic uncertainties between the normalization of the normal and starburst samples are of the order of a factor of 2.

The timescale for perturbation growth can be expressed as $\tau_{\rm grow} \propto (G\rho)^{-0.5}$ (e.g., Larson 1988, 1992; Elmegreen 1994; Wang & Silk 1994), and so $\rho_{\rm SFR} \propto \rho_{\rm gas}/\tau_{\rm grow} \propto \rho_{\rm gas}^{1.5}$. Assuming a constant disk scale height, we obtain equation (3) with $N = 1.5$ for local surface densities. However, disk-averaged quantities will depend on the radial gas distribution. We can also express $\tau_{\rm grow} \sim \alpha\sigma_{\rm gas}/(\pi G\Sigma_{\rm gas}) \sim Q/\kappa$. Perturbation growth via swing amplification in a differentially rotating disk grows in a similar manner (e.g., Larson 1988). By assuming that star formation self-regulates and keeps Q constant, Larson (1988) and Wang & Silk (1994) predict $\Sigma_{\rm SFR} \propto \Sigma_{\rm gas}/\tau_{\rm grow} \propto \Sigma_{\rm gas}\,\Omega$, since $\kappa \propto \Omega$, for disks with flat rotation curves.

However, these theories neglect the effects of magnetic fields and the viscosity of the ISM. Gammie (1996) finds that these significantly reduce the growth rate of non-axisymmetric perturbations for typical Galactic conditions. In the central star-forming disk of NGC 3504, Kenney, Carlstrom, & Young (1993) find $\tau_{\rm grow}$ 3 orders of magnitude shorter than the gas consumption timescale. After accounting for a reasonable star formation efficiency, this discrepancy is still significant. Most Galactic disk stars form in localized, highly clustered regions (Lada, Strom, & Myers 1993) in GMCs, and most of the gas in the disk, including most of the bound gas, is not directly involved in the star formation. In GMCs static magnetic fields play a dynamically important role (e.g., McKee 1999; Heiles et al. 1993). Their presence sets a critical mass,

$$M_B = 512\,\frac{\overline{B}_{1.5}^3}{\overline{n}_{\rm H3}^2}\,M_\odot\,, \tag{5}$$

(Bertoldi & McKee 1992) for spherical clouds, where $\overline{B}_{1.5} \equiv \overline{B}/(10^{1.5}\ \mu{\rm G})$ and $\overline{n}_{\rm H3} \equiv \overline{n}_{\rm H}/10^3\ {\rm cm}^{-3}$. For the diffuse ISM (Elmegreen 1985; Mestel 1985) with $\overline{n}_{\rm H} \sim 1\ {\rm cm}^{-3}$ and $\overline{B} \sim 3\ \mu$G, we have $M_B \sim 5 \times 10^5\ M_\odot$, which is typical for a GMC. Below this mass gravitational collapse is impossible without ambipolar diffusion, and even for greater masses, there will still be a significant effect. Collapse may also be impeded by turbulent magnetic pressure, generated from energy injected by the first stars to form in a cloud. McKee (1999) has modeled these higher mass clouds as being in approximate hydrostatic equilibrium with low-mass star formation providing support. The data supporting the empirical Schmidt laws (eqs. [3] and [4]) are sensitive only to high-mass stars. Since collapse mediated by ambipolar diffusion occurs on a timescale $t_{\rm AD}$, much greater than the free-fall time, $t_{\rm ff}$, we conclude that it is inaccurate to use the rate of purely gravitational perturbation growth of the disk-averaged ISM and, ignoring magnetic fields, to predict global SFRs.

The spatial correlation of star formation with large-scale spiral structure in some disk galaxies motivates theories for the triggering of star formation during the passage of gas through density waves. Wyse (1986) and Wyse & Silk (1989) propose a SFR law of the form

$$\Sigma_{\rm SFR} \propto \Sigma_{\rm gas}^N(\Omega - \Omega_p)\,, \tag{6}$$

where Ω_p is the pattern frequency of the spiral density wave. In the limit of small Ω_p and for $N = 1$, we recover equation

(4). The outer radius of star formation is predicted to be the corotation radius, in approximate agreement with observations. Increased cloud collision rates and increased perturbation growth rates in the arms, where Q is locally lowered, have been suggested as the star formation triggering mechanism. These will be further discussed in § 2.4. Ho, Filippenko, & Sargent (1997) investigate the influence of bar density waves on star formation in the nuclear regions of disk galaxies, finding enhancements in the SFRs of early-type spirals. They argue that this is due to the bar channeling gas to the central region; however, the presence of a bar is neither a necessary nor a sufficient condition for nuclear star formation. The wide range in the strength of nuclear H II regions, whether a bar is present or not, suggests that it is not the passage of gas through a density wave which mediates the star formation rate within a particular starburst.

One prediction of these theories is a correlation of the SFR with the density-wave amplitude. However, this is not observed (Elmegreen & Elmegreen 1986; McCall & Schmidt 1986; K89). Furthermore, such theories have difficulty explaining star formation in galaxies where there is a lack of organized star formation features, as in flocculent spirals (Block et al. 1994; Sakamoto 1996; Thornley & Mundy 1997a, 1997b; Grosbol & Patsis 1998), some of which even contain moderate amplitude density waves as revealed in the near-infrared. GMCs are present, and SFRs are similar to those systems where star formation is organized into spiral patterns. This suggests that stellar disk instabilities, which create spiral density waves, and gas instabilities, which lead to GMCs and large-scale star formation, are decoupled in the sense that one does not cause the other (K89; Seiden & Schulman 1990). This decoupling highlights the need for a theory which physically motivates the Schmidt law of equation (4) without the need for coherent density waves.

In this paper we outline such a theory. The SFR, dominated by stars forming in clustered regions, with high-mass stars present, is controlled by collisions between gravitationally bound gas clouds, which can be atomic, molecular, or both. We find the collision time is a fraction of the orbital period. Collisions create localized, overdense regions where high-mass star formation occurs. The precollision clouds are formed relatively quickly by the action of gravitational, thermal, or Parker instabilities, growing in regions where $Q \lesssim 1$. However, their collapse is halted by static and turbulent magnetic pressure support. The latter may be produced by low-mass star formation regulated by ambipolar diffusion (e.g., McKee 1989), which does not dominate the global galactic SFR. Thus the rate-limiting step for star formation is not the formation of bound clouds but the compression of these, or parts of these, in cloud-cloud collisions. Therefore, at any particular time, most of the bound gas is not undergoing collision-induced star formation. There is no specific need for large-scale, coherent density waves.

There is some evidence for collision-induced star formation in the Galaxy. Scoville, Sanders, & Clemens (1986) noted that the efficiency per unit mass of H_2 for OB star formation decreases significantly with increasing cloud mass over the range 10^5 to $3 \times 10^6\ M_\odot$ (see also § 2.3.3) and concluded that the principal trigger for star formation is not an internal mechanism, such as the growth rate of gravitational instability or sequential star formation. Scoville et al. (1986) suggested that the approximately quadratic dependence of the Galactic H II region distribution on the local H_2 density (averaged on scales of ~ 300 pc) was evidence for cloud collisions causing massive star formation. Detailed observations of individual star-forming regions also suggest that cloud collisions are an important triggering mechanism (Scoville et al. 1986; Maddalena et al. 1986; Hasegawa et al. 1994; Greaves & White 1991; Womack, Ziurys, & Sage 1993). Clouds with embedded clusters of star formation have broader distributions of optical polarization angles than clouds without star formation (Myers & Goodman 1991). This may indicate accumulation of gas at super-Alfvénic speeds in these star-forming regions from the collision of two clouds with distinct magnetic field alignments. Note that the results of Myers & Goodman (1991) suggest the enhanced dispersion in polarization angles is more closely associated with the presence of dense gas than with the young stars which subsequently form. Computer simulations of collisions between inhomogeneous clouds (Klein & Woods 1998) reveal the formation of high-density clumps embedded in filamentary structures, via a bending-mode instability. Such structures are abundant in OMC-1 (Wiseman & Ho 1994, 1996) and Taurus (Ungerechts & Thaddeus 1987). In modeling starbursting systems IC 1908 and NGC 6872, Mihos, Bothun, & Richstone (1993) were unable to reproduce observations of enhanced SFRs in regions of high velocity dispersion and circular velocity gradients, where cloud collision rates are high, with traditional, noncollisional prescriptions of star formation.

While cloud collisions may play an important role in inducing star formation, it is not yet clear whether the majority of star formation is triggered by this process. The data supporting equations (3) and (4) are sensitive only to high-mass star formation, although the bulk of stars are expected to form in these regions (Lada et al. 1993). The theory of collision-induced star formation outlined below requires the initial trigger for most star formation to be a cloud collision. However, subsequent triggering by other processes, such as self-propagating star formation, from the initial site, is not excluded.

The rest of this paper is set out as follows. In § 2.1 we set out our preliminary assumptions, and derive results for gas disks, independent of the hypothesis of collision-induced star formation. In § 2.2 we derive a SFR law of the form $\Sigma_{\rm SFR} \propto \Sigma_{\rm gas}\,\Omega$ in the case of uniform circular velocity, based on star formation from cloud collisions. In § 2.3 we compare this law to observations and make predictions of radial SFR profiles, SFR fluctuations due to different shear velocities, dependencies of disk-averaged SFR with gas density (Schmidt law) and circular velocity (B-band Tully-Fisher relation) and how the efficiency of star formation depends on cloud mass. Such tests are required to distinguish this theory from those involving the growth rate of gravitational perturbations or triggering by density waves. In § 2.4 we examine how large-scale spiral density waves affect the collisional theory. Finally, in § 2.5 we consider the theory's application to the circumnuclear disks of starbursts, which make up most of the dynamic range in the data supporting a global Schmidt law (K98). We conclude in § 3.

2. STAR FORMATION FROM CLOUD COLLISIONS

2.1. *Preliminary Assumptions*

The star-forming regions under consideration are thin, self-gravitating disks. Self-regulated star formation (see, e.g.,

Silk 1997) enforces the condition $Q \sim O(1)$. The circumnuclear disks of starbursts (DS98) and the star-forming regions of disk galaxies (K89) satisfy these conditions. For $Q \lesssim 1$, an overdensity on scales $\sim \lambda_{\rm crit}$ leads to a bound object and we assume that instabilities drive most of the gas mass into bound clouds. Gravitational, Parker, and thermal instabilities have been considered (e.g., Wada & Norman 1999; Burkert & Lin 1999; Elmegreen 1991). The effect of cloud growth via collisional coagulation has also been examined (e.g., Oort 1954; Field & Saslaw 1965; Kwan & Valdes 1987; Das & Jog 1996). Gas in the bound clouds can be either atomic or molecular. In the Milky Way, extended H I envelopes are commonly observed around molecular clouds (e.g., Moriarty-Schieven, Andersson, & Wannier 1997; Williams & Maddalena 1996; Elmegreen 1993; Blitz & Williams 1999). Although Andersson & Wannier (1993) conclude that the H I around low-mass ($\sim 10^3$–10^4 $M_\odot$) clouds is not gravitationally bound, for larger GMCs ($M_c \sim 5 \times 10^5$ $M_\odot$), the situation is probably reversed (L. Blitz 1999, private communication). In the solar neighborhood the mass in atomic envelopes is similar to the mass in GMCs (Blitz 1990). Thus, out to about 8 or 9 kpc, most of the gas in the Galaxy is in self-gravitating clouds. As gas densities and pressures increase toward the centers of galaxies, the molecular fraction of the gas is expected to increase, until it is almost completely molecular in the circumnuclear disks of starbursts (e.g., Liszt & Burton 1996; DS98).

For simplicity we describe the cloud population with a single, typical mass, M_c. In galactic disks, this approximation is justified by the observed mass spectrum of GMCs in the Milky Way, $d\mathcal{N}/dM \propto M^{-\beta}$, with $\beta \sim 1.6$, and with an exponential cutoff above $M_{\rm cut} \sim 5 \times 10^6$ $M_\odot$ (e.g., Solomon et al. 1987). Note that these are only the molecular masses. Most of the gas mass is in the large clouds. Observations suggest that circumnuclear disks are clumpy and the typical mass is much larger (DS98). However, there is little evidence for the form of the mass function. For galactic disks we set $M_c = 5 \times 10^5$ $M_\odot$, while for circumnuclear disks we consider clouds with $M_c = 10^8$ $M_\odot$. The properties and timescales associated with these clouds are shown in Tables 1 and 2.

The cloud radius, r_c, is smaller than its tidal radius, r_t, defined as the radial distance from the cloud's center, at which the shear velocity, v_s, due to differential galactic rotation, is equal to the escape velocity from the cloud at that distance. The shear velocity of two orbits separated by a radial distance, b, is

$$v_s(b) = b\left(\Omega - \frac{dv_{\rm circ}}{dR}\right), \tag{7}$$

and so for $b = r_t$, we have

$$r_t = (1-\beta)^{-2/3}\left(\frac{2M_c}{M_{\rm gal}}\right)^{1/3} R\ . \tag{8}$$

$M_{\rm gal}$ is the galactic mass interior to R, assuming a spherical distribution. This approximation is valid at larger R, when the dark matter halo begins to dominate over the disk mass. For smaller R, and particularly for the circumnuclear disks of starbursts, this is not the case. However, for simplicity, we keep this formalism, where $M_{\rm gal}$ is understood to be the "equivalent interior galactic mass," if the distribution was spherical instead of disklike. Equation (8) implies $r_t \to \infty$ for solid-body rotation, when $dv_{\rm circ}/dR = v_{\rm circ}/R$ and thus $\beta = 1$. For most of the star-forming circumnuclear and galactic disks, rotation curves are flat (DS98; K89), $\beta = 0$, and we have

$$r_t = \left(\frac{2M_c}{M_{\rm gal}}\right)^{1/3} R\ ; \tag{9}$$

r_t is of order 100 pc for the fiducial values of M_c in circumnuclear and galactic disks. The relation between r_c and r_t will be discussed in more detail in § 2.2.

The dimensions of the clouds are comparable to the scale height of the gas disk (e.g., Solomon et al. 1987; DS98), and so we describe the cloud distribution with a thin, two-dimensional disk. We also assume an approximately axisymmetric distribution, so there is a single value of Q at any particular R. Galaxies with strong spiral arms and thus nonaxisymmetric gas distributions will be discussed in § 2.4.

We assume the cloud velocity dispersion, $\sigma_{\rm gas}$, results from a balance of heating via gravitational torquing from noncollisional encounters and cooling via dissipative colli-

TABLE 1

CLOUD PROPERTIES

Property	Formula or Source	Galactic Disk	Circumnuclear Disk
M_c ($M_\odot$).....	M_B (eq. [5]) and observation	$\sim 5 \times 10^5$	$\sim 1 \times 10^{8a}$
R (pc)	Observation	~ 4000	$\sim 600^b$
$v_{\rm circ}$ (km s^{-1}).....	Observation	225	300
r_t (pc)	$(2M_c/M_{\rm gal})^{1/3}R$	~ 100	~ 100
r_c (pc).....	Observation	$\sim 20^c$	$< 100^d$
c_s (km s^{-1}).....	Alfvén velocity	~ 1.5	Uncertain
$v_{\rm rel}$ (km s^{-1})	$\sim 1.6 r_t\Omega + (2GM/r_c)^{1/2}$	13	~ 200
$\bar{n}_{\rm H}$ (cm^{-3})	$0.75M_c/(4\pi r_c^3/3)$	~ 450	$\sim 1.7 \times 10^4$

[a] DS98 are only able to resolve a few of the largest bound clumps, of mass $\sim 10^9$ $M_\odot$, in the circumnuclear disks. By analogy with GMCs in normal disks, we take the typical mass to be an order of magnitude less than this maximum.

[b] This is the mean value of R_1, the inner disk half-intensity (of CO flux) radius, from the sample of DS98.

[c] We take this fiducial value for consistency with the clouds modeled by Gammie et al. 1991. Real clouds of this mass will probably be somewhat more extended, particularly allowing for H I envelopes.

[d] In circumnuclear disks r_c is uncertain. For the calculations that require a definite value, we take $r_c = 35$ pc.

TABLE 2

CLOUD TIMESCALES

PROCESS	FORMULA OR REFERENCE	TIME (yr)	
		Galactic Disk	Circumnuclear Disk
Orbital period, $t_{\rm orb}$	$2\pi R/v_{\rm circ}$	$\sim 110 \times 10^6$	$\sim 12 \times 10^6$
Free-fall, $t_{\rm ff}$	$(3\pi/32G\rho_{\rm gas})^{0.5} \simeq 4.3 \times 10^7 \bar{n}_{\rm H}^{-1/2}$ (yr)	2.0×10^6	0.3×10^6
Atomic to molecular,[a] $t_{\rm conv}$	$\sim 1.6 \times 10^9 n_{\rm H\,I}^{-1}$ (yr)	$\sim 4 \times 10^6$	$\sim 0.1 \times 10^6$
Ambipolar diffusion,[b] $t_{\rm AD}$	$\simeq 15 t_{\rm ff}$ (McKee 1999)	$\gtrsim 30 \times 10^6$	$\gtrsim 5 \times 10^6$
Collision,[c] $t_{\rm coll}$	$\sim (3.2\Omega \mathcal{N}_A r_t^2 f_{\rm G})^{-1} \sim t_{\rm orb}/5$	$\sim 22 \times 10^6$	$\sim 2.4 \times 10^6$
Destruction, $t_{\rm dest}$	Williams & McKee (1997)	$\sim 30 \times 10^6$	Uncertain
Lifetime,[d] $t_{\rm exist}$	$\gtrsim t_{\rm dest} + \min(t_{\rm AD}, t_{\rm coll})$	$\gtrsim 50 \times 10^6$	$\gtrsim 10 \times 10^6$
Alfvén crossing, $t_{\rm cross}$	$2r_c/c_s$	$\simeq 25 \times 10^6$	Uncertain
Impact time, $t_{\rm imp}$	$2r_c/v_{\rm rel}$	$\simeq 2.5 \times 10^6$	$\sim 0.3 \times 10^6$

[a] For $n_{\rm H\,I} = \bar{n}_{\rm H}$ of the cloud.

[b] Note that the estimate of $t_{\rm AD}$ is based on ionization solely from cosmic rays (see McKee 1999, eqs. [2] and [89]). The inhomogeneous nature of interstellar gas clouds means that UV radiation is much more penetrating than in the homogeneous case and that most of the gas mass of clouds is probably at a higher level of ionization, and hence subject to longer ambipolar diffusion timescales, than the above estimate.

[c] This collision timescale is sensitive to the approximation of a cloud population with single cloud mass, M_c. The time between collisions that cause star formation is $f_{\rm sf}^{-1} t_{\rm coll}$.

[d] This is the lifetime of a gravitationally bound cloud, not explicitly a molecular cloud. Upper limits of $\sim 10^8$ yr (e.g., Blitz & Williams 1999) are quoted for GMC lifetimes. However, bound clouds, ignoring the atomic/molecular distinction, may live much longer.

sions. Gammie, Ostriker, & Jog (1991) numerically integrated orbits for two-body encounters to obtain

$$\sigma_{\rm gas} \simeq (GM_c\,\kappa)^{1/3}(1.0 - 1.7\beta)\,, \tag{10}$$

valid for $\beta \ll 1$ and in approximate agreement with Galactic observations (e.g., Stark & Brand 1989; Knapp, Stark, & Wilson 1985; Clemens 1985). For a flat rotation curve, this is approximately the shear velocity of an encounter of impact parameter $b = r_t$. The surface densities of real disks, set by $Q \sim O(1)$, are such that the effects of many-body interactions may be important. N-body simulations are required to probe these effects. Substituting for $\sigma_{\rm gas}$ in equation (1), we derive the radial distribution of gas,

$$\begin{aligned}\Sigma_{\rm gas} &= \frac{\alpha\kappa^{4/3} M_c^{1/3}}{\pi G^{2/3} Q} \\ &\propto M_c^{1/3}\left(\frac{v_{\rm circ}}{R}\right)^{4/3} \frac{(1+\beta)^{2/3}(1.0 - 1.7\beta)}{Q} \\ &\propto \frac{M_c^{1/3} v_{\rm circ}^{4/3}(1 - 1.0\beta)}{R^{4/3} Q}\,. \end{aligned} \tag{11}$$

Note that K89 assumed $\sigma_{\rm gas}$ was independent of R, which leads to an underestimation of Q, by factors of a few, in the central galactic regions, compared to the case where equation (10) is used instead. This may explain the slight trend of Q decreasing by factors of a few as one moves toward the centers of galaxies (see K89, Fig. 11), rather than remaining constant. However, better statistics are required before a proper comparison can be made.

When $Q \gg 1$, the assumption that most of the gas mass is organized in bound clouds breaks down, together with our use of equation (10). The presence of a large-scale stellar bar, channeling gas radially inward, will deplete the gas from certain regions, thus raising Q. Here we expect little or no star formation. This may be the situation in the inner few kiloparsecs of the Milky Way (e.g., Binney et al. 1991).

2.2. *The Collision-induced SFR*

Our principal hypothesis is that cloud collisions, by compressing parts of the clouds, induce the majority of star formation in galactic and circumnuclear disks. However, collisions can also be disruptive. A simple theoretical condition for colliding clouds to remain bound has been given by Larson (1988). Neglecting postshock cooling, the clouds stay bound if the ram pressure, $\sim \rho_c v_{\rm rel}^2$, is less than the binding pressure, $\sim G\Sigma_c^2$, where ρ_c and Σ_c are the cloud volume and surface densities, respectively. For typical galactic disk cloud properties in Table 1, this implies $\Sigma_c \gtrsim 900\ M_\odot\ {\rm pc}^{-2}$, which is higher than the mean value for GMCs ($\sim 170\ M_\odot\ {\rm pc}^{-2}$) by a factor of about 5. Realistic clouds are probably more extended, with a gradually decreasing density profile. Interactions in these outer layers reduce the actual relative velocity from the value quoted in Table 1. Radiative postshock cooling reduces the disrupting pressure, and thus also relaxes the above condition. Therefore we expect some collisions to lead to an increase in mass, density, and the gravitational potential energy of the clouds involved, and hence the likelihood of faster SFRs.

The outcome of cloud collisions has also been investigated numerically (e.g., Lattanzio et al. 1985), but the simulations have usually been unable to resolve the Jeans length, thus violating the numerical Jeans condition (Truelove et al. 1997). Furthermore, there has been no systematic attempt to probe the parameter space of cloud collisions, as defined by the angle of collision, impact parameter, Mach number, and mass ratio. Magnetic fields have yet to be included. For the idealized cases considered, the results of a collision depend sensitively on the collision parameters (R. Klein 1999, private communication; Lattanzio et al. 1985). We make the simplifying assumption that the fraction of a cloud converted into stars in a typical collision, averaging over the parameter space of possible collisions, is constant.

We consider the thin disk of self-gravitating clouds described in § 2.1, where $Q \sim O(1)$. We hypothesize that $\Sigma_{\rm SFR}$ is, on average, inversely proportional to the collision

time, $t_{\rm coll}$, of these clouds. A fraction, ϵ, of each gas cloud is converted into stars in each burst of collision-induced star formation. The time between bursts is $f_{\rm sf}^{-1} t_{\rm coll}$, where $f_{\rm sf}$ is the fraction of collisions which lead to star formation. Thus,

$$\Sigma_{\rm SFR} = \frac{\epsilon f_{\rm sf} \mathcal{N}_A M_c}{t_{\rm coll}} \simeq \frac{\epsilon f_{\rm sf} \Sigma_{\rm gas}}{t_{\rm coll}} , \quad (12)$$

where $\mathcal{N}_A$ is the surface number density of gravitationally bound clouds per unit area of the disk. By numerically solving the equations of motion, Gammie et al. (1991, Fig. 8), found that cloud-cloud collisions result from encounters caused by differential rotation, primarily with initial impact parameters of about $1.6 r_t$, and with a spread in values of order r_t.[1] For typical GMC parameters in the Galaxy, the associated shear velocity is ~ 9 km s^{-1}. This sets the collision rate, together with the cloud surface density, $\mathcal{N}_A$, and the probability of collision, $f_{\rm G}$, of these encounters. Note that the random velocity dispersion of the cloud population (~ 7 km s^{-1}; see, e.g., Stark & Brand 1989) sets the clouds moving on epicycles but is not the velocity directly influencing the collision rate. The effect of these random motions has been accounted for in the calculations of Gammie et al., since they consider the collision of clouds that are already moving on epicycles. Increasing the random motions increases the initial impact parameters at which most cloud collisions occur, raising the shear velocity and thus the collision rate. We express $t_{\rm coll}$ as

$$t_{\rm coll} \sim \frac{1}{2} \frac{\lambda_{\rm mfp}}{v_s(\sim 1.6 r_t)} \sim \frac{1}{3.2 r_t (\Omega - dv_{\rm circ}/dR) \mathcal{N}_A r_t f_{\rm G}} , \quad (13)$$

where the first factor of $\frac{1}{2}$ accounts for clouds either catching up with others at larger R or being caught up with by clouds at smaller R. $\lambda_{\rm mfp} = 1/\mathcal{N}_A r_t f_{\rm G}$ is the mean free path of a cloud to catch up, or be caught up to, by another. The denominator $v_s(\sim 1.6 r_t) \simeq 1.6 r_t (\Omega - dv_{\rm circ}/dR)$ is the shear velocity of an encounter with impact parameter $\sim 1.6 r_t$, due to differential rotation.

We evaluate the factor $\mathcal{N}_A r_t^2$ via

$$\mathcal{N}_A \simeq \frac{\Sigma_{\rm gas}}{M_c} = \frac{\alpha \kappa \sigma_{\rm gas}}{\pi G Q M_c} \simeq (1 + 0.3\beta) \frac{0.7\alpha}{Q r_t^2} . \quad (14)$$

As in equation (11), we have used $\kappa = \sqrt{2}\Omega(1+\beta)^{1/2}$ and assumed the velocity dispersion of the gas clouds results from gravitational torquing (Gammie et al. 1991), so that $\sigma_{\rm gas} \simeq (G M_c \kappa)^{4/3} (1.0 - 1.7\beta)$, with $\beta \ll 1$. So $\mathcal{N}_A \pi r_t^2 = (1 + 0.3\beta) 0.7\alpha\pi/Q \sim O(1)$ and is constant where Q is constant. Thus every area element, πr_t^2, of the disk approximately contains the mass of gas, M_c, required to set r_t. Thus, from equation (13),

$$t_{\rm coll} \simeq \frac{Q}{9.4 f_{\rm G} (1 + 0.3\beta)(1 - \beta)} t_{\rm orb} . \quad (15)$$

From Gammie et al. (1991) we set $f_{\rm G} \sim 0.5$. We expect it to scale as r_c/r_t. We consider cloud boundaries to be set by pressure confinement from the general ISM pressure, $P_{\rm ISM}$. Following Elmegreen (1989), we have

$$P_{\rm ISM} \simeq \frac{\pi}{2} G \Sigma_{\rm gas} \left(\Sigma_{\rm gas} + \Sigma_* \frac{\sigma_{\rm gas}}{\sigma_*} \right) , \quad (16)$$

where Σ_* and σ_* are the stellar surface density and velocity dispersion, respectively. The boundary pressure of the self-gravitating clouds is a few times less than the interior cloud pressure, $P \sim \frac{1}{2} G \Sigma_c^2$, where $\Sigma_c \simeq M_c/\pi r_c^2$. Since $Q \sim O(1)$ implies $\Sigma_{\rm gas} \simeq M_c/\pi r_t^2$, and with $P \sim P_{\rm ISM}$, we have

$$\frac{r_c}{r_t} = \left(\frac{\Sigma_{\rm gas}}{\Sigma_c} \right)^{1/2} \sim \left[\frac{\Sigma_{\rm gas}}{\Sigma_{\rm gas} + \Sigma_* (\sigma_{\rm gas}/\sigma_*)} \right]^{1/4} . \quad (17)$$

Observationally, $\Sigma_{\rm gas}$ and Σ_* have approximately similar spatial distributions, and so from equation (17) we see that r_c/r_t, and thus $f_{\rm G}$, varies only very slowly with R. From here on we take it to be a constant.

Substituting equation (15) in equation (12), we obtain

$$\Sigma_{\rm SFR} \simeq 1.5 \epsilon f_{\rm sf} f_{\rm G} Q^{-1} \Sigma_{\rm gas} \Omega (1 - 0.7\beta) . \quad (18)$$

This is a new "modified" Schmidt law, to be tested against observations (§ 2.3). For our fiducial location in the Galactic disk ($R = 4$ kpc) we have

$$\Sigma_{\rm SFR} \simeq 4.3 \times 10^{-8} M_\odot \ {\rm yr}^{-1} \ {\rm pc}^{-2} \left(\frac{\epsilon}{0.2} \frac{f_{\rm sf}}{0.5} \frac{f_{\rm G}}{0.5} \frac{1.0}{Q} \right) \times \left[\frac{\Sigma_{\rm gas}}{10 \ M_\odot \ {\rm pc}^{-2}} \frac{\Omega}{5.7 \times 10^{-8} \ {\rm yr}^{-1}} (1 - 0.7\beta) \right] . \quad (19)$$

Disk-averaged SFRs, with the appropriate gas distribution, are estimated in § 2.3.2.

2.3. *Predictions of Collision-induced Star Formation*

2.3.1. *Radial Profiles*

With high-resolution data for $\Sigma_{\rm SFR}$, $\Sigma_{\rm gas}$, including atomic and molecular components, and $v_{\rm circ}$, equation (18) can be directly tested. This is practical for the Milky Way and nearby galaxies, but difficult for circumnuclear disks of starbursts because of their small size. Star formation from cloud collisions is a stochastic process and so statistically significant data sets are required. Properly identifying bound clouds requires atomic and molecular observations, so the masses of both components can be accounted for.

The assumption that the cloud velocity dispersion is caused by gravitational torquing (Gammie et al. 1991), also leads to the prediction of $\Sigma_{\rm gas}(R)$ (eq. [11]). Combining this with equation (18) leads to

$$\Sigma_{\rm SFR}(R) \propto M_c^{1/3} \Omega^{7/3} Q^{-2} (1 - 1.7\beta) , \quad (20)$$

which is proportional to $M_c^{1/3} R^{-7/3} Q^{-2}$ for constant $v_{\rm circ}$. If observations of $\Sigma_{\rm gas}$ are lacking, then the theory can still be tested using equation (20) and SFR and circular velocity data, for an assumed constant Q. Note that $M_c(R)$ is, in general, difficult to determine. However, surveys of Galactic CO (e.g., Sanders et al. 1986) find no strong evidence for systematic variation (Solomon et al. 1987; Scoville et al. 1987). Furthermore, any variation is weakened by being raised to the $\frac{1}{3}$ power in equation (20). If galactic stellar disks have been built up primarily through self-regulated star formation, where $Q \sim O(1)$, then we also have $\Sigma_* \propto \Sigma_{\rm SFR}$ as an additional prediction.

Several authors have presented radial profiles of $\Sigma_{\rm gas}$ and $\Sigma_{\rm SFR}$ for individual galaxies (e.g., Tacconi & Young 1986; Kuno et al. 1995). However, problems of accounting for the varying extinction of the tracers of star formation, such as Hα, make direct comparison difficult. Similarly, where far-infrared emission is used as a SFR estimator, the heating contributions from young stars, old stars, and possible

[1] The length unit used in Gammie et al. (1991) corresponds to $\sim 0.8 r_t$.

AGN activity must be disentangled. A follow-up paper (Martin & Kennicutt 2000, in preparation) to K98 will present radial data for many galaxies, accounting for these effects.

One distinct prediction of this theory results from the extra dependence of the SFR on variations in the circular velocity. Statistically, we expect negative velocity gradients in the rotation curve to increase the SFR and positive gradients to decrease it. Regions of solid body rotation will be free of collisions resulting from shearing motions. Thus we expect star formation here to have its rate controlled by a different process, such as ambipolar diffusion.

Within the star-forming regions of disks, we expect a positive correlation between the SFR and the velocity dispersion of the clouds. With higher random velocities they move on larger epicycles, and encounters with greater initial impact parameters and greater shear velocities occur, leading to increased collision rates.[2] No such prediction is made by the theory of star formation triggered by the rate of gas passage through spiral arms. In a future paper we plan to investigate this question with high-resolution BIMA and VLA data.

2.3.2. *Disk Averages: Schmidt Law and Tully-Fisher Relation*

We also test equation (18) by examining the disk-averaged properties of galaxies and starbursts. We note, however, that such tests, while good consistency checks, do not discriminate well between the different theories of how star formation is triggered. We take the area-weighted mean of equation (18) over the whole region of a disk, where $Q \sim 1$ and $v_{\rm circ}$ is constant, to obtain

$$\overline{\Sigma_{\rm SFR}} \equiv \frac{1}{\pi(R_2^2 - R_1^2)} \int_{R_1}^{R_2} \Sigma_{\rm SFR}(R) 2\pi R\, dR = 1.5 \epsilon f_{\rm sf} f_{\rm G} \overline{\Sigma_{\rm gas} \Omega} \,. \quad (21)$$

Current observations do not have the spatial resolution to estimate $\overline{\Sigma_{\rm gas}\Omega}$, except for the nearest galaxies. However, K98 presents data revealing a correlation between $\overline{\Sigma_{\rm SFR}}$ and $\overline{\Sigma_{\rm gas}}\,\Omega_2$, where Ω_2 is the angular rotation frequency at the outer radius, R_2, of the star-forming region (Fig. 2). Since we are considering the flat rotation curve case, we rewrite equation (21) as

$$\overline{\Sigma_{\rm SFR}} = 1.5 \epsilon f_{\rm sf} f_{\rm G} \Omega_2 R_2 \left(\frac{\overline{\Sigma_{\rm gas}}}{R} \right) . \quad (22)$$

For $\Sigma_{\rm gas} \propto R^{-4/3}$ (eq. [11]) we obtain

$$\overline{\Sigma_{\rm SFR}} = 3 \epsilon f_{\rm sf} f_{\rm G} \Omega_2 \overline{\Sigma_{\rm gas}} \left(\frac{x^{-1/3} - 1}{1 - x^{2/3}} \right) , \quad (23)$$

where $x = R_1/R_2$, R_1 being the inner radius where the rotation curve is flat. If x is uncorrelated with Ω_2 and $\overline{\Sigma_{\rm gas}}$, then we predict K98's observed correlation.

Applying equation (23) to the inner 8.5 kpc of the Milky Way, assuming $x = 0.2$ and $\epsilon = 0.2$ (see § 2.3.3), gives

$$\mathrm{SFR}_{\rm tot} = \overline{\Sigma_{\rm SFR}} \pi R_2^2 = 1.6\ M_\odot\ \mathrm{yr}^{-1} \times \left(\frac{R_2}{8.5\ \mathrm{kpc}} \frac{v_{\rm circ}}{225\ \mathrm{km\ s^{-1}}} \frac{\overline{\Sigma_{\rm gas}}}{10\ M_\odot\ \mathrm{pc}^{-2}} \right) \times \left(\frac{\epsilon}{0.2} \frac{f_{\rm sf}}{0.5} \frac{f_{\rm G}}{0.5} \frac{1.0}{Q} \right) . \quad (24)$$

This is consistent with estimates based on observations of thermal radio emission from H II regions, which give $\mathrm{SFR}_{\rm tot} = 2.7 \pm 0.9\ M_\odot\ \mathrm{yr}^{-1}$ (Güsten & Mezger 1982; McKee 1989). Scaling to a typical starbursting circumnuclear disk, with $R_2 = 1.7$ kpc, $v_{\rm circ} = 300$ km s^{-1} and $\overline{\Sigma_{\rm gas}} = 10^3\ M_\odot\ \mathrm{pc}^{-2}$, gives $\mathrm{SFR}_{\rm tot} = 42\ M_\odot\ \mathrm{yr}^{-1}$. One of the most uncertain factors in these estimates is $f_{\rm sf}$. Numerical studies (R. Klein 1999, private communication), although not yet incorporating magnetic fields, can constrain this number.

We also predict the form of the B-band Tully-Fisher relation, $L_B \propto v_{\rm circ}^{\alpha_{\rm TF}}$. Assuming $L_B \propto \overline{\Sigma_{\rm SFR}} R_2^2$, we have

$$L_B \propto v_{\rm circ} R_2 \overline{\Sigma_{\rm gas}} \propto v_{\rm circ}^{7/3} R_2^{-1/3} M_c^{1/3} , \quad (25)$$

where we have evaluated $\overline{\Sigma_{\rm gas}}$ using equation (11), assuming $R_1 \ll R_2$. This result compares favorably with the observed B-band exponent of $\alpha_{\rm TF} \simeq 2.1$–$2.2$ (Burstein et al. 1995; Strauss & Willick 1995). The Tully-Fisher relation at longer wavelengths becomes more and more contaminated by light from older stellar populations.

2.3.3. *Cloud Star Formation Efficiency*

Collision-induced star formation predicts a variation in the star formation efficiency, ϵ, of GMCs, dependent on their mass. Variations in ϵ, resulting from this and other mechanisms, have been considered by a number of authors (e.g., Elmegreen & Clemens 1985; Scoville et al. 1986; Pandey, Paliwal, & Mahra 1990; Franco, Shore, & Tenorio-Tagle 1994; Ikuta & Sofue 1997; Williams & McKee 1997).

Scoville et al. (1986) found the ratios of Lyman-continuum luminosity to M_c and number of high-luminosity H II regions to M_c decreased with increasing M_c. They argued this was evidence for collision-induced star formation, since, if the collision rate scaled as the cloud surface area ($\propto M_c^{2/3}$), then the efficiency of star formation per unit cloud mass, ϵ, would scale as $M_c^{-1/3}$. However, if a more appropriate mass-size relationship ($M_c \propto r_c^2$; Larson 1981) is applied with their reasoning, then no scaling of ϵ with M_c is predicted.

Ikuta & Sofue (1997) considered the (radio) luminosity of H II regions, rather than simply the number, associated (less than 10 pc away in the plane of the sky) with molecular clouds. They found $\epsilon \propto M_c^{-0.78}$. However, they did not allow for higher mass clouds being larger than smaller ones. The centers of large clouds may be much farther than 10 pc away from H II regions associated with their periphery. There is also no comment on the completeness of the data. In particular, the H II region sample, being flux limited at 1 Jy, is incomplete below luminosities of $\sim$250 Jy kpc^2 for sources in the inner Galaxy.[3]

We now revisit the question of how the efficiency, $\epsilon \equiv M_*/(M_* + M_c) \simeq M_*/M_c$, of star formation depends on cloud mass. Observationally, we measure ϵ by summing the radio luminosity, $L_{\rm rad}$, of H II regions associated with a cloud. This luminosity is converted into a stellar mass using $M_* = 570 S_{49}\ M_\odot = 6.84 L_{\rm rad}\ M_\odot\ \mathrm{Jy}^{-1}\ \mathrm{kpc}^2$ (McKee & Williams 1997). Dividing by M_c then gives ϵ. We use the H II region data of Downes et al. (1980) and the molecular

[2] Complications arise if the likelihood of star formation changes significantly with the increase in relative velocity of the collision. Numerical simulations are required to investigate this effect.

[3] A luminosity of 1 Jy kpc^2 $\simeq 0.012 S_{49}$, where S_{49} is the ionizing luminosity ($\lambda < 912$ Å) in units of 10^{49} photons s^{-1}. For example, Orion A has $S_{49} = 2.7$ and $L = 230$ Jy kpc^2. Note that by definition an object with a radio flux of 1 Jy at a distance of 1 kpc has a luminosity of 1 Jy kpc^2, i.e., there is no factor of 4π.

cloud data of Solomon et al. (1987). For each of the 106 H II regions, with resolved distance ambiguity, in the same region as the cloud survey, molecular clouds within $40(M_c/5 \times 10^5\ M_\odot)^{1/2}$ pc (i.e., $2r_c$) on the sky, within the correct radial distance bounds and with relative velocities of less than 15 km s^{-1} are identified. The H II region is associated with the closest cloud, if more than one is identified. With these criteria, 83 H II regions are associated with 39 clouds. These data are shown in Figure 3*a*, with the typical errors shown by the cross.

However, there are also two issues of completeness for the sample. First, as already mentioned, the H II data are incomplete for $L < 250$ Jy kpc^2. We adopt the more conservative limit of 400 Jy kpc^2, which is shown by the diagonal dashed line in Figure 3*a*. The data below this line are incomplete. Second, the molecular cloud data are incomplete for $M_c \lesssim 4 \times 10^5\ M_\odot$ (Williams & McKee 1997). This is shown by the vertical dashed line. Assuming, for a particular M_c, that the probability of detection of a cloud is uncorrelated with $L_{\rm rad}$, we ignore the effect of cloud incompleteness in the following analysis. The total $L_{\rm rad}$ for each cloud is recalculated, now only summing individual H II regions with $L_{\rm rad} > 400$ Jy kpc^2. This data is shown in Figure 3*b*. The best-fit straight line is shown by the long dashed line.

We now compare these observations with theory. We model a cloud of mass M_c, with H II regions, as resulting from a binary collision of two smaller clouds of masses M_1 and M_2, with $M_1 + M_2 = M_c$ and $M_1 < M_2$. The assumption of binary collisions is justified by the paucity of high-mass star formation in the total cloud population. Given our lack of understanding of the detailed results of cloud collisions, the assumption that several H II regions, rather than just one, may result from a single collision event is reasonable. M_1 (and M_2) are chosen from the mass spectrum of clouds: $d\mathcal{N}/dM \propto M^{-\beta}$, with $\beta \sim 1.6$. Following our original hypothesis applied to equal-mass clouds, that, on average, in a collision a constant fraction, ϵ, of the total

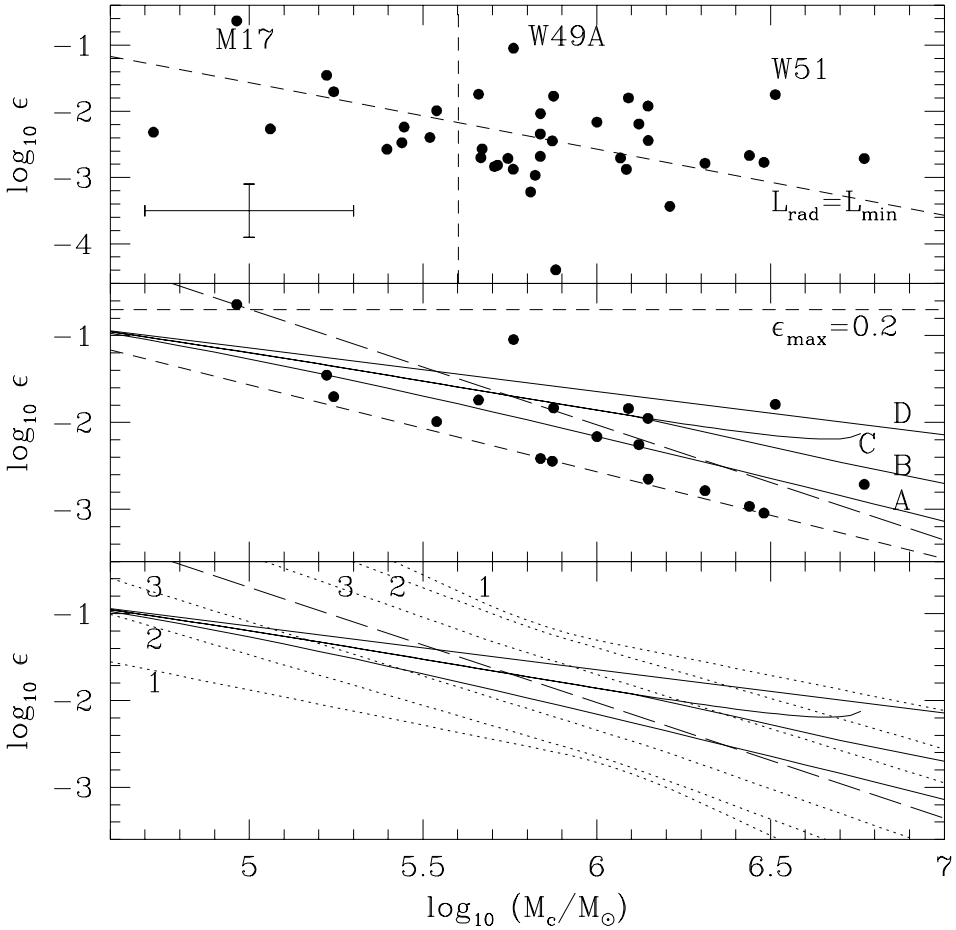

FIG. 3.—Star formation efficiency, ϵ, vs. cloud mass, M_c. *Top:* Full sample of 39 clouds associated with 83 H II regions. The cross shows typical errors of 0.3 in $\log_{10} M_c$ and 0.4 in $\log_{10}\epsilon$. The diagonal dashed line shows the efficiency a cloud would have if associated with an H II region of luminosity $L_{\rm min} = 400$ Jy kpc^2. The data are incomplete below this line. The vertical dashed line shows the molecular cloud survey completeness boundary at $M_c = 4 \times 10^5\ M_\odot$ (Williams & McKee 1997). *Middle:* Complete sample of 19 clouds associated with individual H II regions, each with $L_{\rm rad} > L_{\rm min}$. The completeness boundary is again shown by the diagonal dashed line. The adopted value of $\epsilon_{\rm max} = 0.2$ is shown by the horizontal dashed line. The best linear fit to this data in logarithmic space is shown by the long-dashed line. Solid lines show various model predictions: (A) collision-induced star formation; (B) stochastic star formation (Williams & McKee 1997); (C) stochastic star formation with $\epsilon_{\rm max}(M)$ = constant; (D) uniform distribution of ϵ in logarithmic space. *Bottom:* 95% confidence intervals on the best linear fit (*long-dashed line*) to the data in logarithmic space are shown by the dotted lines: (1) limit for the existing 19 data points, with errors shown by cross in the top panel; (2) limit for hypothetical data set of 190 clouds with the same distribution as the existing 19; (3) limit for these 190 clouds with typical errors half of those shown by cross in the top panel. Note that although these limits are based on the (poor) assumption of a normal distribution of the data about the best-fit line, and are only limits on linear fits (hence the deviation at low M_c), this figure still illustrates that with 10 times more data and with errors reduced by a factor of 2, one can hope to distinguish between the different models (*solid lines*, as in the middle panel).

cloud mass forms stars, we assume for unequal mass collisions that the mass of stars formed is $2\epsilon M_1$. Thus $L_{\rm rad} \propto M_1$, and the maximum star formation efficiency, $\epsilon_{\rm max}$, is statistically achieved for collisions of equal-mass clouds ($M_1 = M_c/2$), and is thus independent of M_c. From the data in Figure 3*b*, we set $\epsilon_{\rm max} = 0.2$. The observationally determined minimum luminosity, above which the H II region sample is complete, defines a minimum value, $M_{\rm min}$, for M_1. Thus $M_{\rm min} < M_1 < M_c/2$. These two constraints meet when $M_{\rm min} = M_c/2$, and thus the star formation efficiency data for a complete sample of H II regions associated with clouds will be contained within a triangular region in a diagram of $\log \epsilon$ versus $\log M_c$ (Fig. 3*b*).

The typical value of M_1, $\langle M_1 \rangle$, is an average of M_1 weighted by the collision rate. This scales with M_c via

$$\langle M_1 \rangle = \frac{\int_{M_{\rm min}}^{M_c/2} M_1 \, t_{\rm coll}^{-1}(M_1) dM_1}{\int_{M_{\rm min}}^{M_c/2} t_{\rm coll}^{-1}(M_1) dM_1} \propto M_c^{0.4} , \quad (26)$$

in the region where $M_{\rm min} \ll M_c$, since from equation (13), we have

$$t_{\rm coll}^{-1}(M_1) \propto \mathcal{N}_{A,\rm sum} r_{t,\rm sum}^2 \propto M_1^{-1.6} , \quad (27)$$

and since $r_{t,\rm sum} = r_{t,1} + r_{t,2} \propto M_c^{1/3}$ is approximately independent of M_1, and $\mathcal{N}_{A,\rm sum} = \mathcal{N}_{A,1} + \mathcal{N}_{A,2} \simeq \mathcal{N}_{A,1} \propto M_1^{-1.6}$. Thus $\langle M_1 \rangle \propto M_c^{0.4}$, and so

$$\langle \epsilon \rangle = 2\epsilon \langle M_1 \rangle / M_c \propto M_c^{-0.6} . \quad (28)$$

Performing an averaging of the distribution of M_1 (and thus ϵ) given by equation (26), in logarithmic space, leads to line A in Figure 3*b*.

We also consider three other theoretical models for comparison. Models B and C (stochastic star formation; Williams & McKee 1997) assume a cloud's star formation rate is linearly proportional to its mass, provided $\epsilon_{\rm max}$ is not exceeded. Model B imposes a mass dependence, at high masses, on $\epsilon_{\rm max}$ by assuming there is a physical limit to the maximum luminosity of OB associations. Model C assumes $\epsilon_{\rm max}$ is independent of M_c, and the observed maximum association luminosity is simply the result of sparse sampling of the distribution. By normalizing to the observed Galactic OB association luminosity and molecular cloud mass functions, a probability distribution of association luminosities expected in a cloud of mass M_c, approximately proportional to L^{-2} is predicted. After summing the expected number of associations in a cloud, and then averaging the resulting distribution of ϵ at each M_c in logarithmic space, we obtain lines B and C. Finally we consider an unphysical model (D) with a uniform distribution of $\log \epsilon$ for clouds of a particular mass.

The four model predictions are shown in Figures 3*b* and 3*c*. In the latter, we also show the 95% confidence limits[4] on (1) the linear best fit from the existing sample, (2) a hypothetical sample 10 times larger with the same distribution, and (3) as for (2) but with individual measurement errors reduced by a factor of 2. From the existing data, model D is marginally excluded (because of its slope), while A, B, C are all consistent. Although the confidence limits on fitting a nonlinear function will differ in detail, Figure 3*c* qualitatively shows that with 10 times more data and with modest improvements in measurement accuracy, we can hope to discriminate between these models. Such a sample can be achieved by a survey of radio H II regions in the entire inner Galaxy to fluxes of order 0.1 Jy. Improving completeness of CO observations of smaller mass GMCs will also improve the statistics. Uncertainties in M_c result from the assumption of virialization and the CO/H_2 ratio. Errors in $L_{\rm rad}$ result in part from distance uncertainties. Direct infrared observations of massive stars may improve estimates of association luminosities.

As a final point of caution, we note that evolutionary effects will cause a cloud's measured ϵ to change. At the onset of star formation ϵ will be small, while ϵ will increase as the cloud is destroyed by energy injection from its high-mass stars. Large enough samples are required to average over this effect.

In summary, collision-induced star formation predicts a decrease in the mean cloud star formation efficiency of a complete sample with increasing cloud mass. The decrease occurs since it is much more likely for a large cloud to suffer a collision with a smaller one, because of the cloud mass spectrum. It is the smaller cloud which then determines the amount of resultant star formation. An observational lower limit to H II region luminosities, included in the analysis, implies a constant minimum mass of the smaller cloud, which drives the mass dependence of ϵ. Stochastic models predict a similar, but less steep, decline due to the shape of the complete region in the ϵ versus M_c parameter space. For stochastic models, at high cloud masses, if $\epsilon_{\rm max}$ is independent of M_c,[5] the efficiencies tend toward a constant value. Improved data samples should allow for discrimination between the models.

2.4. *Effects of Spiral Density Waves*

The theory for collision-induced star formation requires modification where there is a tight spatial correlation of star formation with spiral structure. Spiral density waves decrease the local value of Q, and often $Q < 1$ in the arm region and $Q > 1$ in the interarm region (e.g., Kuno et al. 1995). Two scenarios are possible. In the first, the rate-limiting step is the formation of bound clouds, occurring exclusively in the arms, after which the clouds form stars at a fast rate (e.g., via gravitational collapse of magnetically supercritical clouds or through rapid collisions) and all the bound gas is involved in star formation. Equation (6) is then a better description of the galactic SFR. In the second scenario, bound cloud formation is fast and is not the rate-limiting step. A reservoir of bound gas clouds exists in the galaxy, including in the interarm regions. Spiral arms now act to concentrate the spatial distribution of gas clouds, and the collision rate is enhanced in the arms. The individual collision rate for a particular cloud is still described by equation (13), but the overall SFR is modulated by the length of time the gas clouds spend in the arm region (related to $\Omega - \Omega_p$ and the width and pitch angle of the arm) and the degree of spatial concentration of clouds in the arm (related to the strength of the spiral density wave).

The similarity of the global star-forming properties of galaxies with and without large-scale density waves argues

[4] Based on the assumption of a normal distribution of data about the best-fit line. The limits on acceptable slopes of fits are shown by the asymptotic limit of these confidence limits. Fits with more extreme slopes but still within the boundaries are also excluded.

[5] A new physical regime may be reached at very high cloud masses in the extreme conditions of circumnuclear starbursting disks, when the ionized gas is no longer able to escape from the cloud. This will have a profound effect on the efficiency of star formation. The analysis of this section can thus only be applied to clouds in "normal" galactic environments.

against bound cloud formation being controlled exclusively by spiral arms (see § 1). Deciding which scenario is the correct description, or if both processes operate at some level, requires study of the arm to interarm gas distributions and cloud collision timescales in larger samples of galaxies, which exhibit a tight correlation of star formation with spiral arms. Obviously, neither scenario can explain the star formation observed in the galaxies without strong spiral structure.

2.5. *Application to Circumnuclear Disks of Starbursts*

The $\Sigma_{\rm SFR}$ and $\Sigma_{\rm gas}$ data of the circumnuclear disks of starbursts make up most of the dynamic range for K98's Schmidt law relationships (Figs. 1 and 2). However, much less is known about the details of this star formation compared to that occurring in the outer regions of galactic disks.

Downes & Solomon (1998) present observations and models of 10 circumnuclear disks. Their key findings, relevant to the theory of collision-induced star formation are the following: most of the circumnuclear disks are in the flat rotation curve regime;[6] $Q \sim O(1)$; the disks are thin and modeled without need to invoke large-scale nonaxisymmetric features, such as bars or spiral arms; much of the star formation is associated with very large bound gas clouds with maximum masses $\sim 10^9\ M_\odot$ and sizes (~ 100 pc) consistent with their confinement by tidal shear forces. Thus our principal assumptions are met.

The gas disks are predominantly molecular, including the intercloud medium, with the gas mass approximately $\frac{1}{6}$ of the dynamical mass. Note, that larger gas masses (by a factor of ~ 5) are derived if the standard $\rm CO/H_2$ conversion factor for virialized GMCs in normal galaxies is used (as in the analysis of K98). In fact, much of the CO luminosity of the circumnuclear disks comes from the nonvirialized molecular intercloud medium.

Since $Q \sim O(1)$ and not $\ll 1$, the gas is probably not collapsing on the free-fall timescale ($t_{\rm ff} < 10^6$ yr). This is consistent with Downes & Solomon's estimate that about half the gas is converted into stars over 10 orbital periods ($\sim 100 \times 10^6$ yr). This efficiency per orbital period is similar to that of normal galactic disks (K98), motivating a unified theory to describe both regimes. The collision time for a typical cloud mass, which we take to be of order $10^8\ M_\odot$, is a few million years.

The one inconsistency between our theory and the results of DS98, is their estimate that only $\sim 10\%$ of the gas mass is in bound clouds. They base this estimate on observations of HCN which requires densities $\sim 10^5\ \rm cm^{-3}$ for excitation. However, the fact that $Q \sim 1$ implies that any overdense region on the critical scales will become gravitationally bound. A large fraction of the gas may be at densities less than that required for strong HCN emission, and yet still in bound clouds.

Circumnuclear starburst disks and the star-forming regions of normal galactic disks may represent the extremes of a continuous family of states. Our theory of collision-induced star formation can be applied in both situations. As one moves inward from the outer disk, the gas surface densities and the molecular fractions of the bound clouds increase, but self-regulation of star formation maintains $Q \sim O(1)$. The typical cloud mass, M_c, also appears to increase. If this is set by the magnetic critical mass, M_B, of the intercloud medium, then, from equation (5), $\overline{B}^3/\overline{n}^2$ must increase as R decreases. The typical cloud mass may also be affected by changes in the collision time. This is much shorter ($\sim 2.4 \times 10^6$ yr) in circumnuclear disks than in the typical star-forming locations of normal disks ($\sim 22 \times 10^6$ yr), particularly in comparison to the stellar evolutionary and cloud destruction timescales. This may increase M_c in circumnuclear disks to be several times M_B.

[6] This includes most of the gas mass. Although the data are limited, most of the star formation as traced by the "extreme starburst events" (DS98, Table 12) is also in this regime. The mean rotation curve turn over radius is 220 pc, the mean half–CO intensity radius is 630 pc, and the mean outer disk boundary (used in the disk average analysis of K98) is 1.7 kpc.

3. CONCLUSIONS

We have invoked star formation triggered by cloud-cloud collisions to explain global star formation rates in disk galaxies and circumnuclear starbursts. The theory predicts a scaling of SFR with $\overline{\Sigma}_{\rm gas}$ and Ω_2 in agreement with the observations of K98. For reasonable parameter values it also predicts the correct normalization of the scaling law, although estimates are uncertain. Previous theories based on the growth rate of gravitational perturbations ignore the dynamically important presence of magnetic fields. Theories based on triggering by spiral density waves fail to explain star formation in systems without such waves. Furthermore, observations suggest that gas and stellar disk instabilities are decoupled.

Star formation resulting from cloud collisions has been proposed in the past (e.g., Scoville et al. 1986) but rejected because of supposedly long collision timescales. However, Gammie et al. (1991) show that the collision rate of self-gravitating particles in a differentially rotating disk is much larger than that of particles in a box. Collision rates are enhanced because particles collide at the shear velocity of encounters with initial impact parameters of order two tidal radii (typically a few hundred parsecs for GMCs). Also, the small scale height of GMCs implies essentially two-dimensional interactions in the plane of the disk, increasing the collision rate relative to that for three dimensions. We calculate collision timescales short enough to allow a viable theory of collision-induced star formation to be considered.

In summary, in this model, self-gravitating gas disks fragment into bound gas clouds. This process is driven either by gravitational, thermal, or Parker instabilities, or the influence of stellar spiral density waves on the gas. These bound clouds, either atomic or molecular, are relatively long-lived, being supported by static and turbulent magnetic pressure. The latter may be produced by dynamically regulated low-mass star formation (McKee 1999). We hypothesize that a fraction of cloud collisions lead to compression of localized regions of the clouds. These regions, if magnetically supercritical, collapse rapidly to form stars, including high-mass OB stars. The bulk of Galactic disk stars are thought to form via this "burst"-mode (Lada et al. 1993). Thus, the rate-limiting step for star formation is not the formation of bound clouds, but the compression of these, or parts of these, in cloud-cloud collisions. Therefore, at any particular time, most of the bound gas is not actively undergoing star formation.

Specifically, we have considered an idealized, single-mass population of gravitationally bound gas clouds, orbiting in an axisymmetric, thin disk. Using the result of Gammie et al. (1991) for the cloud velocity dispersion, we predict radial gas distributions, dependent on the Toomre Q stability

parameter (eq. [11]). Applying our principal hypothesis, that cloud collisions trigger the majority of disk star formation, using the collision cross section results of Gammie et al. (1991) and with the assumption that star formation self-regulates ($Q \sim O(1)$), we predict enhanced cloud collision rates and a SFR law of the form $\Sigma_{\rm SFR}(R) \simeq 1.5\epsilon f_{\rm sf} f_{\rm G} Q^{-1} \Sigma_{\rm gas} \Omega(1 - 0.7\beta)$ (eq. [18]). For flat rotation curves ($\beta = 0$), this result is in agreement with the disk-averaged data of K98 (Fig. 2). Although uncertain, our estimates of the total SFR in the Milky Way and for typical starburst systems are consistent with observations. We predict a B-band Tully-Fisher relation of the form $L_B \propto v_{\rm circ}^{7/3}$, in agreement with observations (Burstein et al. 1995; Strauss & Willick 1995).

This theory is to be further scrutinized to discriminate between it and other star formation mechanisms. To this end we have proposed several tests. We predict statistically enhanced SFRs in regions of large negative circular velocity gradients, where the shear rate is increased, and regions of increased cloud velocity dispersion. Similarly, decrements are predicted in regions of large positive circular velocity gradients, which reduce the amount of shear. Future observations (Martin & Kennicutt 2000, in preparation) of SFR, gas, and circular velocity profiles of large samples of disk galaxies should allow for statistically significant tests of our proposed SFR law, and in particular the dependence on the circular velocity gradients and cloud velocity dispersion. However, these tests will be complicated by possible variations in the likelihood of collision-induced star formation with collision velocity. The results of numerical simulations may be necessary to account for this effect. We also predict that star formation efficiency, ϵ, linearly averaged, decreases with increasing cloud mass as $\langle \epsilon \rangle \propto M_c^{-0.6}$. Figure 3 shows model predictions for ϵ, logarithmically averaged over its distribution, and comparison with observations. Larger and deeper surveys of H II regions and GMCs, including their atomic components, are required to improve the significance of this test.

Undoubtedly our model is an extremely simplified description of the actual star formation process. We have presented an idealized theory in which all star formation is triggered by cloud collisions; however, other processes, such as spontaneous star formation, self-triggering, and triggering by density waves undoubtedly operate at some level. For the results of the collision-induced theory to be valid, we require that the majority of (high-mass) star formation is initially triggered by this process. The basic theory needs modification where there is a tight correlation of star formation with large-scale density waves, allowing for the duration clouds spend in the density wave and the degree of spatial concentration.

The theory can be improved by numerical calculation of collision rates in a many-body system, rather than relying on simple two-body interaction rates. Numerical simulation of cloud collisions (e.g., Klein & Woods 1998) may provide insight into the details of how a magnetically supercritical region can be produced from the collision of two magnetically subcritical clouds. The parameter space for the outcome of collisions with different initial conditions is also being probed by simulation (R. Klein 1999, private communication). These simulations will constrain the probability, $f_{\rm sf}$, for star formation to result from typical cloud-cloud collisions.

This theory can be applied to analytic models (e.g., Shore & Ferrini 1995) and simulations (e.g., Curir & Mazzei 1998; Weil, Eke, & Efstathiou 1998) of disk galaxy formation and evolution, for comparison with cosmological SFR data.

We thank Chris McKee for many hours of stimulating discussion and much input. We also thank Leo Blitz, Andrew Cumming, Alex Filippenko, Rob Kennicutt, Richard Klein, Crystal Martin, Chris Matzner, Antonio Parravano, Evan Scannapieco, Joe Silk, Tony Wong, and an anonymous referee for helpful comments. My research is supported in part by a grant from the NSF (AST 95-30480).

REFERENCES

Andersson, B.-G., & Wannier, P. G. 1993, ApJ, 402, 585
Bertoldi, F., & McKee, C. F. 1992, ApJ, 395, 140
Binney, J., Gerhard, O. E., Stark, A. A., Bally, J., & Uchida, K. I. 1991, MNRAS, 252, 210
Blitz, L. 1990, The Evolution of the Interstellar Medium, ed. L. Blitz (San Francisco: ASP), 273
Blitz, L., & Williams, J. P. 1999, in Conf. Proc. on the Physics of Star Formation and Early Stellar Evolution (Crete II), preprint (astro-ph/9903382)
Block, D. L., et al. 1994, A&A, 288, 365
Burkert, A., & Lin, D. N. C. 1999, ApJ, submitted
Burstein, D., et al. 1995, in The Opacity of Spiral Disks, ed. J. I. Davies & D. Burstein (Dordrecht: Kluwer), 73
Clemens, D. P. 1985, ApJ, 295, 422
Curir, A., & Mazzei, P. 1998, New Astron., 4, 1
Das, M., & Jog, C. J. 1996, ApJ, 462, 309
Downes, D., & Solomon, P. M. 1998, ApJ, 507, 615 (DS98)
Downes, D., Wilson T. L., Bieging, J., & Wink, J. 1980, A&AS, 40, 379
Elmegreen, B. G. 1985, in Protostars and Planets II, ed. D. Black & M. Matthews (Tucson: Univ. Arizona Press), 33
———. 1989, ApJ, 338, 178
———. 1991, ApJ, 378, 139
———. 1993, ApJ, 411, 170
———. 1994, ApJ, 425, L73
Elmegreen, B. G., & Clemens, C. 1985, ApJ, 294, 523
Elmegreen, D. M., & Elmegreen, B. G. 1986, ApJ, 311, 554
Field, G. B., & Saslaw, W. C. 1965, ApJ, 142, 568
Franco, J., Shore, S. N., & Tenorio-Tagle, G. 1994, ApJ, 436, 795
Gammie, C. F. 1996, ApJ, 462, 725
Gammie, C. F., Ostriker, J. P., & Jog, C. J. 1991, ApJ, 378, 565
Greaves, J. S., & White, G. J. 1991, A&A, 248, L27
Grosbol, P. J., & Patsis, P. A. 1998, A&A, 336, 840
Güsten, R., & Mezger, P. G. 1982, Vistas Astron., 26, 159
Hasegawa, T., Sato, F., Whiteoak, J. B., & Miyawaki, R. 1994, ApJ, 429, L77
Heiles, C., Goodman, A. A., McKee, C. F., & Zweibel, E. G. 1993, in Protostars and Planets III, ed. E. H. Levy & J. I. Lunine (Tucson: Univ. Arizona Press), 279
Ho, L. C., Filippenko, A. V., & Sargent, W. L. W. 1997, ApJ, 487, 591
Ikuta, C., & Sofue, Y. 1997, PASJ, 49, 323
Jog, C. J. 1996, MNRAS, 278, 209
Jog, C. J., & Solomon, P. M. 1984, ApJ, 276, 114
Kenney, J. D. P., Carlstrom, J. E., & Young, J. S. 1993, ApJ, 418, 687
Kennicutt, R. C. 1989, ApJ, 344, 685 (K89)
———. 1998, ApJ, 498, 541 (K98)
Klein, R. I., & Woods, D. T. 1998, ApJ, 497, 777
Knapp, G. R., Stark, A. A., & Wilson, R. W. 1985, AJ, 90, 254
Kuno, N., Nakai, N., Handa, T., & Sofue, Y. 1995, PASJ, 47, 745
Kwan, J., & Valdes, F. 1987, ApJ, 315, 92
Lada, E. A., Strom, K. M., & Myers, P. C. 1993, in Protostars and Planets III, ed. E. H. Levy & J. I. Lunine (Tucson: Univ. Arizona Press), 245
Larson, R. B. 1981, MNRAS, 194, 809
———. 1988, in Galactic and Extragalactic Star Formation, ed. R. E. Pudritz & M. Fich (Dordrecht: Kluwer), 435
———. 1992, in Star Formation in Stellar Systems, ed. G. Tenorio-Tagle, M. Prieto, & F. Sanchez (Cambridge: Cambridge Univ. Press), 125
Lattanzio, J. C., Monaghan, J. J., Pongracic, H., & Schwarz, M. P. 1985, MNRAS, 215, 125
Liszt, H. S., & Burton, W. B. 1996, in Unsolved Problems of the Milky Way, ed. L. Blitz & P. Teuben (Dordrecht: Kluwer), 297
Maddalena, R. J., Morris, M., Moscowitz, J., & Thaddeus, P. 1986, ApJ, 303, 375
McCall, M. L., & Schmidt, F. H. 1986, ApJ, 311, 548
McKee, C. F. 1989, ApJ, 345, 782

McKee, C. F. 1999, in The Origin of Stars and Planetary Systems, ed. C. J. Lada & N. D. Kylafis (Dordrecht: Kluwer), 29
McKee, C. F., & Williams, J. P. 1997, ApJ, 476, 144
Mestel, L. 1985, in Protostars and Planets II, ed. D. Black & M. Matthews (Tucson: Univ. Arizona Press), 320
Mihos, J. C., Bothun, G. D., & Richstone, D. O. 1993, ApJ, 418, 82
Moriarty-Schieven, G. H., Andersson, B.-G., & Wannier, P. G. 1997, ApJ, 475, 642
Myers, P. C., & Goodman, A. A. 1991, ApJ, 373, 509
Oort, J. H. 1954, Bull. Astron. Inst. Netherlands, 12, 177
Pandey, A. K., Paliwal, D. C., & Mahra, H. S. 1990, ApJ, 362, 165
Quirk, W. J. 1972, ApJ, 176, L9
Sakamoto, K. 1996, ApJ, 471, 173
Sanders, D. B., Clemens, D. P., Scoville, N. Z., & Solomon, P. M. 1986, ApJS, 60, 1
Schmidt, M. 1959, ApJ, 129, 243
Scoville, N. Z., Sanders, D. B., & Clemens, D. P. 1986, ApJ, 310, L77
Scoville, N. Z., Yun, M. S., Clemens, D. P., Sanders, D. B., & Waller, W. H. 1987, ApJS, 63, 821
Seiden, P. E., & Schulman, L. S. 1990, Adv. Phys., 39, 1
Shore, S. N., & Ferrini, F. 1995, Fundam. Cosmic Phys., 16, 1
Silk, J. 1997, ApJ, 481, 703
Solomon, P. M., Rivolo, A. R., Barrett, J., & Yahil, A. 1987, ApJ, 319, 730
Spitzer, L. 1978, Physical Processes in the Interstellar Medium (New York: Wiley)
Stark, A. A, & Brand, J. 1989, ApJ, 339, 763
Strauss, M. A., & Willick, J. A. 1995, Phys. Rep., 261, 272
Tacconi, L. J., & Young, J. S. 1986, ApJ, 308, 600
Taniguchi, Y., & Ohyama, Y. 1998, ApJ, 509, L89
Thornley, M. D., & Mundy, L. G. 1997a, ApJ, 484, 202
———. 1997b, ApJ, 490, 682
Toomre, A. 1964, ApJ, 139, 1217
Truelove, J. K., Klein, R. I., McKee, C. F., Holliman, J. H., Howell, L. H., & Greenough, J. A. 1997, ApJ, 489, L179
Ungerechts, H., & Thaddeus, P. 1987, ApJS, 63, 645
Wada, K., & Norman, C. 1999, ApJ, 516, L13
Wang, B., & Silk, J. 1994, ApJ, 427, 759
Weil, M. L., Eke, V. R., & Efstathiou, G. 1998, MNRAS, 300, 773
Williams, J. P., & Maddalena, R. J. 1996, ApJ, 464, 247
Williams, J. P., & McKee, C. F. 1997, ApJ, 476, 166
Wiseman, J., & Ho, P. T. P. 1994, in ASP Conf. Ser. 65, Clouds, Cores and Low Mass Stars, ed. D. P. Clemens & R. Barvainis (San Francisco: ASP), 396
———. 1996, Nature, 382, 139
Womack, M., Ziurys, L. M., & Sage, L. J. 1993, ApJ, 406, L29
Wyse, R. F. G. 1986, ApJ, 311, L41
Wyse, R. F. G., & Silk, J. 1989, ApJ, 339, 700